Acta Crystallographica Section C
Crystal Structure Communications
ISSN 0108-2701

Luminescence properties of the structure built from 3-cyano-4-dicyanomethylene-5-oxo-4,5-dihydro-1*H*-pyrrol-2-olate and caesium(I)

Viktor A. Tafeenko,* Stanislav I. Gurskiy, Marat F. Fazylbekov, Andrey N. Baranov and Leonid A. Aslanov

Chemistry Department, Moscow State University, 119899 Moscow, Russian Federation
Correspondence e-mail: viktor@struct.chem.msu.ru

Received 14 December 2009
Accepted 22 December 2009
Online 8 January 2010

The structure of caesium(I) 3-cyano-4-dicyanomethylene-5-oxo-4,5-dihydro-1*H*-pyrrol-2-olate (Cs*A*), $Cs^{+}\cdot C_8HN_4O_2^{-}$, is related to its luminescence properties. The structure of Cs*A* (triclinic, $P\overline{1}$) is not isomorphous with previously reported structures (monoclinic, $P2_1/c$) of the K*A* and Rb*A* salts. Nevertheless, the coordination numbers of the metals are equal for all salts (nine). Each anion in the Cs*A* salt is connected by pairs of inversion-related N—H···O hydrogen bonds to another anion, forming a centrosymmetric dimer. The dimers are linked into infinite ribbons, stacked by means of π–π interactions, thus building up an anionic wall. Time-dependent density functional theory calculations show that the formation of the dimer shifts the wavelength of the luminescence maximum to the blue region. Shortening the distance between stacked anions in the row [from 3.431 (5) Å for Rb*A* to 3.388 (2) Å for K*A* to 3.244 (10) Å for Cs*A*] correlates with a redshift of the luminescence maximum from 574 and 580 nm to 596 nm, respectively.

Comment

Establishing the correlation between physical properties of individual molecules and their crystals is essential in the search for new materials. In the present paper, we study the correlation between the structure (Fig. 1) and luminescence properties of the caesium salt, (I), of 3-cyano-4-dicyanomethylene-5-oxo-4,5-dihydro-1*H*-pyrrol-2-olate (*A*). It was shown in a previous report (Tafeenko *et al.*, 2009) that the luminescence spectra of three salts of *A* with alkali metals (Na, K and Rb) in solution do not depend on the nature of the cation but correlate with the dielectric constant of the solvent. In the solid state, the luminescence maximum (λ max) varies with structural parameters: the redshift of the maximum of luminescence increases with a decrease of the distance between the stacked anions. It was also shown that in the isostructural potassium and rubidium salts all exocyclic heteroatoms of *A* are involved in the formation of a nearly ideal tricapped trigonal prism that encloses the cation, and the anions are arranged in stacks as a result of π–π interactions. The caesium cation has a larger ionic radius than the potassium and rubidium cations, so replacing potassium or rubidium by caesium in the tricapped trigonal prism allows us to enlarge its volume and the distance between adjacent anions in the stack. According to our previous results, a blueshift in the luminescence spectrum of the salt was expected. Contrary to expectations, the luminescence spectrum of the caesium salt in the solid state showed a maximum at 596 nm, *viz.* it is redshifted compared with the potassium (λ max = 580 nm) and the rubidium (λ max = 574 nm) salts.

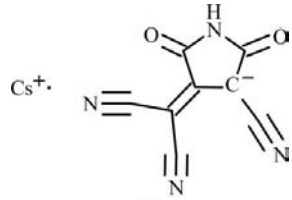

(I)

In the Cs*A* salt, as in the Rb*A* and K*A* salts, the coordination number of the metal is nine and all external atoms of anion *A* are involved in the formation of the coordination polyhedron. However, the coordination polyhedron for caesium could hardly be classified as a tricapped trigonal prism because it does not contain any parallel faces (see Fig. 2). Each polyhedron is connected to a neighboring polyhedron *via* a common, nearly rectangular, face, thus forming double polyhedra. Coupled polyhedra are connected by four edges to neighboring polyhedra to form a layer lying in the *ab* plane (Fig. 3). The shortest distance between cations in the coupled polyhedra is 4.5860 (11) Å [Cs1···Cs1^{iv}; symmetry code: (iv) $-x, -y+1, -z$], while the shortest distances between cations located in different double polyhedra are 5.0909 (11) [Cs1···Cs1^{vii}; symmetry code: (vii) $-x, -y, -z$] and 5.8737 (12) Å [Cs1···Cs1^{iii}; symmetry code: (iii) $-x+1, -y+1,$

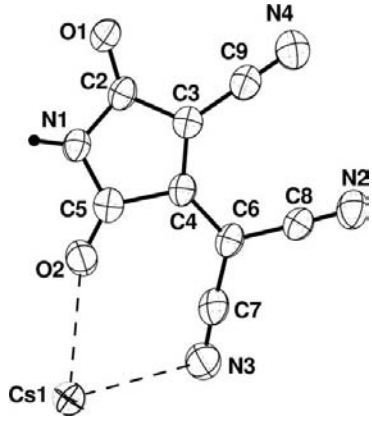

Figure 1
The atom-numbering scheme in the title caesium salt, with displacement ellipsoids drawn at the 50% probability level.

  doi:10.1107/S0108270109055097

$-z$]. The cation–apex distances in the polyhedron vary in the range 3.157 (5)–3.527 (9) Å. These values are much larger than the values of 2.833 (1)–3.173 (2) Å reported for the potassium salt and 2.964 (2)–3.271 (3) Å for the rubidium salt. Each anion is linked by two N1—H1···O1^{viii} [N1···O1 = 2.850 (9) Å, H1···O1^{viii} = 2.00 Å and N1—H1···O1^{viii} = 171°; symmetry code: (viii) $-x$, $-y+2$, $-z+1$] hydrogen bonds to another anion, thus forming a centrosymmetric dimer. Adjacent dimers are connected by –CN···NC– dipole–dipole and π–π interactions, thus forming infinite essentially planar ribbons (Fig. 4). Since each ribbon interacts with two adjacent ribbons by means of π–π interactions, we may consider the dimers to be molecular building blocks of anionic walls (Fig. 4). The ribbons of adjacent walls are parallel, in contrast to the crystal structure of the ammonium salt (Tafeenko *et al.*, 2005), where ribbons of adjacent walls form a dihedral angle of 53.70 (4)°. The distance between the anions in the stacks of the caesium salt is 3.244 (10) Å. This value is shorter than the corresponding distances in the potassium and rubidium salts [3.388 (2) and 3.431 (5) Å, respectively]. The correlation between these values and the luminescence maximum wavelength is clear – the shorter the distance, the larger the redshift of the luminescence maximum (574, 580 and 596 nm for the rubidium, potassium and caesium salts, respectively). However, in contrast to the structures of the potassium and rubidium salts, *A* anions in the structure of the caesium salt form centrosymmetric dimers by means of N—H···O hydrogen bonding. Hydrogen bonding may alter the luminescence properties of the salts in the solid state.

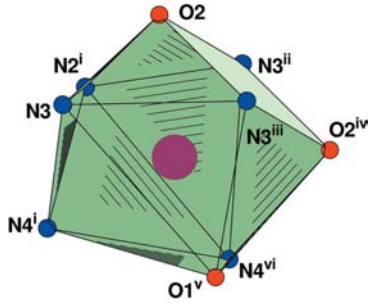

Figure 2
The polyhedron surrounding a Cs^+ cation, showing the deviation from a tricapped trigonal–prismatic geometry. The coordination number of the caesium cation is nine. [Symmetry codes: (i) $-x+1$, $-y+1$, $-z+1$; (ii) $x-1$, y, z; (iii) $-x+1$, $-y+1$, $-z$; (iv) $-x$, $-y+1$, $-z$; (v) x, $y-1$, $z-1$; (vi) $x-1$, $y-1$, $z-1$.]

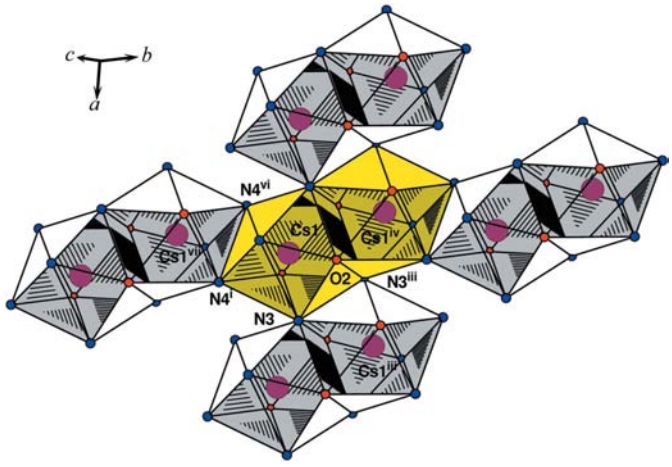

Figure 3
Part of the crystal structure showing how polyhedra coupled by common faces are connected by the edges N3/N3^{iii} and N4^{i}/N4^{vi}, thus forming an essentially planar layer lying in the *ab* plane. The cations lie within 0.082 (1) Å of the least-squares plane. The shortest distances between cations are listed in the *Comment*. [Symmetry codes: (i) $-x+1$, $-y+1$, $-z+1$; (iii) $-x+1$, $-y+1$, $-z$; (iv) $-x$, $-y+1$, $-z$; (vi) $x-1$, $y-1$, $z-1$; (vii) $-x$, $-y$, $-z$.]

The effect of hydrogen bonding on the luminescence spectrum maximum was clarified by means of quantum-chemistry methods. The monomer *A*, $C_8HN_4O_2^-$, and the centrosymmetric dimer $[C_8HN_4O_2^-]_2$ were taken as models to study. (Because of the time-consuming computing procedure and for simplicity, the sodium cation was chosen instead of caesium as counter-ion.) We used density functional theory (DFT) for the ground-state (S_0) and time-dependent density functional theory (TDDFT; Bauernschmitt & Ahlrichs, 1996) for the excited-state (S_n) equilibrium structure optimization and vertical transition energy calculations between excited and ground states of the monomer and dimer (computational details are described in the *Experimental* section). Vertical excitation energies and oscillator strengths for singlet–singlet $S_0 \rightarrow S_n$ transitions are listed in Table 1. It was found that the $S_0 \rightarrow S_1$ and $S_0 \rightarrow S_3$ transitions with high oscillator strength may be attributed to the optically allowed excitation electronic transitions for the monomer and the dimer, respectively. We calculated the equilibrium configurations of the nuclear skeleton of the S_1 and S_3 states for the monomer and the dimer. The vertical transition energies and oscillator strengths of the $S_1 \rightarrow S_0$ and $S_3 \rightarrow S_0$ transitions for the monomer S_1 state and dimer S_3 state of an equilibrium structure are listed in Table 2. In addition, we optimized the S_1-state and S_2-state equilibrium structures of the dimer and evaluated the $S_1 \rightarrow S_0$ and $S_2 \rightarrow S_0$ transition energies. These values correspond to the IR range of the spectrum. However, it was shown experimentally that the luminescence maxima of both the caesium and the sodium salts are in the visible range of the spectrum. Consequently, the luminescence of both the

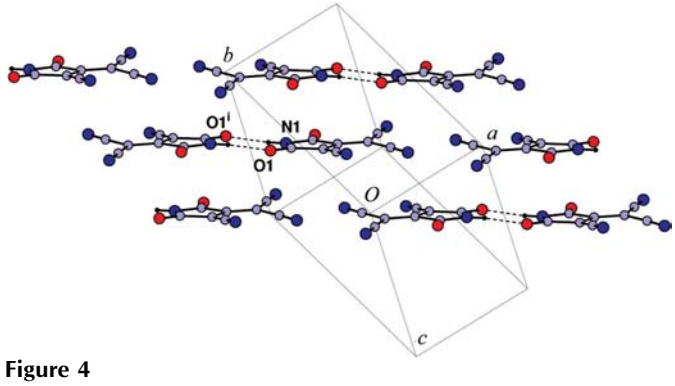

Figure 4
The arrangement of the centrosymmetric anionic dimers (blocks) in ribbons. Adjacent blocks in each ribbon are connected by –CN···NC– dipole–dipole and π–π interactions. Adjacent ribbons are interconnected *via* π–π interactions, forming an anionic wall. The interplanar distance is 3.18 (1) Å. Hydrogen-bonding parameters are listed in the *Comment*.

caesium and the sodium salts corresponds to the $S_3 \rightarrow S_0$ transition in dimers composed of *A* anions. The data presented in Table 2 show that, for the dimer, the $S_3 \rightarrow S_0$ transition is blueshifted by 56.8 nm compared with the monomer $S_1 \rightarrow S_0$ transition.

Therefore, formation of the centrosymmetric dimer of *A* anions *via* hydrogen bonding results in a significant blueshift effect on the luminescence maximum. The formation of dimers in the crystal structure diminishes the effect of redshift caused by π–π interaction between stacking anions. However, for the Cs*A* salt, the π–π 'stacking effect' prevails over the 'dimers effect', resulting in a redshift of the luminescence maximum value of 16 nm relative to that of the K*A* salt.

Experimental

The title salt was obtained by mixing the alkali caesium iodide, CsI, in aqueous solution with a suspension of 2,2,3,3-tetracyanocyclopropanecarboxylic acid in propan-2-ol, in a 1:1 molar ratio. The reaction was carried out at room temperature, and the water and propan-2-ol *v*/*v* ratio was taken as 1:1. An orange powder was obtained from the reaction mixture after solvent evaporation, and this was washed with diethyl ether and dissolved in a water–ethanol mixture (1:1 *v*/*v*). The resulting solution was left aside at 318 K. Upon slow evaporation over a period of 7 d, dark-red crystals of the title caesium salt were obtained.

Crystal data

$Cs^+ \cdot C_8HN_4O_2^-$
M_r = 318.04
Triclinic, $P\overline{1}$
a = 5.8737 (9) Å
b = 9.2927 (11) Å
c = 9.6759 (11) Å
α = 113.040 (11)°
β = 90.834 (13)°
γ = 100.401 (12)°
V = 475.90 (11) Å^3
Z = 2
Mo $K\alpha$ radiation
μ = 3.87 mm^{-1}
T = 295 K
0.08 × 0.06 × 0.05 mm

Data collection

Enraf–Nonius CAD-4 diffractometer
Absorption correction: part of the refinement model (ΔF) (Walker & Stuart, 1983)
T_{min} = 0.084, T_{max} = 0.538
2424 measured reflections
2290 independent reflections
1665 reflections with $I > 2\sigma(I)$
R_{int} = 0.047
2 standard reflections every 60 min
intensity decay: none

Refinement

$R[F^2 > 2\sigma(F^2)]$ = 0.053
$wR(F^2)$ = 0.134
S = 1.04
2290 reflections
137 parameters
H-atom parameters constrained
$\Delta\rho_{max}$ = 0.93 e Å^{-3}
$\Delta\rho_{min}$ = −1.75 e Å^{-3}

Atom H1 was treated as riding on the parent (N1) atom, with an N1—H1 distance of 0.86 Å and a U_{iso}(H1) value of 1.2U_{eq}(N1). For DFT and TDDFT calculations, we used the B3LYP (Becke, 1993) exchange–correlation functional with the 6–311++G** (Krishnan *et al.*, 1980; McLean & Chandler, 1980) basis set. Calculations were performed with *PC GAMESS*/*Firefly* (Granovsky, 2008) and the *GAMESS* (US) *QC* packages (Schmidt *et al.*, 1993) for the DFT and TDDFT methods, respectively.

Data collection: *CAD-4 Software* (Enraf–Nonius, 1989); cell refinement: *CAD-4 Software*; data reduction: *XCAD4* (Harms & Wocadlo, 1995); program(s) used to solve structure: *SHELXS97* (Sheldrick, 2008); program(s) used to refine structure: *SHELXL97* (Sheldrick, 2008); molecular graphics: *DIAMOND* (Brandenburg, 2000); software used to prepare material for publication: *SHELXL97*.

Table 1
Vertical transitions of the monomer and dimer at the ground-state equilibrium geometries (TDDFT/B3LYP/6–311++G**).

Molecule	Transition	Energy (eV)	Wavelength (nm)	Oscillator strength
Monomer	$S_0 \rightarrow S_1$	2.672	464.0	0.184
	$S_0 \rightarrow S_2$	3.374	367.5	0.001
	$S_0 \rightarrow S_3$	3.660	338.8	0.000
	$S_0 \rightarrow S_4$	4.246	292.0	0.000
	$S_0 \rightarrow S_5$	4.562	271.8	0.112
Dimer	$S_0 \rightarrow S_1$	2.562	483.9	0.000
	$S_0 \rightarrow S_2$	2.581	480.4	0.000
	$S_0 \rightarrow S_3$	2.674	463.7	0.416
	$S_0 \rightarrow S_4$	2.718	456.2	0.000
	$S_0 \rightarrow S_5$	3.630	341.6	0.000

Table 2
Vertical transitions of the monomer at the S_1 state equilibrium geometry and the dimer at the S_3 state equilibrium geometry (TDDFT/B3LYP/6–311++G**).

Molecule	Transition	Energy (eV)	Wavelength (nm)	Oscillator strength
Monomer	$S_1 \rightarrow S_0$	2.097	591.2	0.114
Dimer	$S_3 \rightarrow S_0$	2.320	534.4	0.112

We thank the Russian Foundation for Basic Research for financial support (grant No. ofi-08-03-12109) and Dr Denis I. Grigorashev for assistance in the luminescence spectra measurements. All quantum-chemical calculations were performed on cluster MIPT-60 at the Moscow Institute of Physics and Technology.

Supplementary data for this paper are available from the IUCr electronic archives (Reference: FG3147). Services for accessing these data are described at the back of the journal.

References

Bauernschmitt, R. & Ahlrichs, R. (1996). *Chem. Phys. Lett.* **256**, 454–464.
Becke, A. D. (1993). *J. Chem. Phys.* **98**, 5648–5652.
Brandenburg, K. (2000). *DIAMOND*. Release 2.1d. Crystal Impact GbR, Bonn, Germany.
Enraf–Nonius (1989). *CAD-4 Software*. Version 5.0. Enraf–Nonius, Delft, The Netherlands.
Granovsky, A. A. (2008). *PC GAMESS/Firefly*. Version 7.1.F. http://classic.chem.msu.su/gran/gamess/index.html.
Harms, K. & Wocadlo, S. (1995). *XCAD4*. University of Marburg, Germany.
Krishnan, R., Binkley, J. S., Seeger, R. & Pople, J. A. (1980). *J. Chem. Phys.* **72**, 650–654.
McLean, A. D. & Chandler, G. S. (1980). *J. Chem. Phys.* **72**, 5639–5648.
Schmidt, M. W., Baldridge, K. K., Boatz, J. A., Elbert, S. T., Gordon, M. S., Jensen, J. H., Koseki, S., Matsunaga, N., Nguyen, K. A., Su, S., Windus, T. L., Dupuis, M. & Montgomery, J. A. (1993). *J. Comput. Chem.* **14**, 1347–1363.
Sheldrick, G. M. (2008). *Acta Cryst.* A**64**, 112–122.
Tafeenko, V. A., Gurskiy, S. I., Baranov, A. N., Kaisarova, T. V. & Aslanov, L. A. (2009). *Acta Cryst.* C**65**, m52–m55.
Tafeenko, V. A., Peschar, R., Kajukov, Y. S., Kornilov, K. N. & Aslanov, L. A. (2005). *Acta Cryst.* C**61**, o366–o368.
Walker, N. & Stuart, D. (1983). *Acta Cryst.* A**39**, 158–166.